

Nonlinear Finite Element Method in Crashworthiness Analysis of Aircraft Seats

Akif O. Bolukbasi*

Simula Inc., Tempe, Arizona
and

David H. Laananen†

Arizona State University, Tempe, Arizona

A three-dimensional mathematical model of an aircraft seat, occupant, and restraint system has been developed for use in the analysis of light aircraft crashworthiness. Because of the significant role played by the seat in overall system crashworthiness, a detailed finite element model of the seat structure is included. The seat model can accommodate large displacements, nonlinear material behavior, and local buckling. The occupant model consists of 12 rigid mass segments whose dimensions and inertial properties have been determined from studies of human body anthropometry and kinematics and from measurements of anthropomorphic test dummies. Model predictions are compared with measured data from dynamic tests of a simple seat.

Introduction

THERE are three major considerations in designing crashworthiness into a vehicle structure. The first is to ensure that sufficient living space is maintained during impact. The second is to restrain the occupant to prevent injurious contact with the vehicle's interior or ejection from it; implicit in this requirement is the need to retain the seat in the vehicle as well as to keep the occupant in the seat. Third, the forces experienced by the occupant should be attenuated to a tolerable level.¹

A number of dynamic models of the human body have been developed for use in crash survivability analysis. These models vary in complexity and possess from 1 to 40 degrees of freedom. One-dimensional models have been used in prediction of human body response to an ejection seat firing, which, with the body tightly restrained, is an essentially one-dimensional phenomenon. However, an aircraft crash generally also involves a horizontal component of deceleration, which forces rotation of body segments with respect to each other. If no lateral component of deceleration is present, a two-dimensional model will suffice, provided that the restraint system is symmetric. The diagonal shoulder belt, that, combined with a lap belt, forms the standard automotive restraint system and is the one most likely to be used in light aircraft, is asymmetric and may cause lateral motion of the occupant even in the absence of a lateral deceleration. Therefore, a model that is to be useful in restraint system evaluation should be capable of predicting three-dimensional motion. Two-dimensional models made up of interconnected rigid links are described in Refs. 2 and 3, and three-dimensional models in Refs. 4-8.

Except for the two-dimensional PROMETHEUS, described in Ref. 2, the above programs were developed primarily for use in evaluation of automobile interior design, and the seat has been represented in a very simple manner. However, the peak vertical acceleration present in an aircraft accident often exceeds the level that the human body can tolerate in a

direction parallel to the spine. In light aircraft and helicopters it is seldom practical to consider designing sufficient energy-absorbing capacity into the lower airframe structure to protect against these vertical forces, since the crush space is generally not available. Therefore, the seat must play an important role in the crashworthiness of these aircraft. In a crash environment the seat structures may experience large plastic deformations as well as local buckling of tubular members, and prediction of the seat structure response to dynamic loads presents a complex engineering problem.

In this paper, SOM-LA (seat occupant model-light aircraft), a digital computer program developed for use in analysis of light aircraft seats and restraint systems, is described. The program combines a dynamic model of the human body with a finite element model of the seat structure. It is intended to provide the design engineer with a tool for analyzing the structural elements of the seat as well as evaluating the dynamic response of the occupant during a crash.

The original model was described in Ref. 9. A number of modifications have been made to the model since then to improve simulation quality and add desirable output. Several testing programs have been conducted to provide data for validation of the mathematical model, and the final model and its validation are described in Ref. 10. The purpose of this paper is to describe the model, particularly the features of the structural analysis, and one of its validation test programs.

Occupant Model

The three-dimensional occupant model consists of 12 rigid segments, as shown in Fig. 1. The midtorso, lower neck, shoulder, and hip joints are ball-and-socket type, each possessing three rotational degrees of freedom. The upper neck, elbow, and knee joints are hinge-type joints, each adding one degree of freedom. In total, the occupant system possesses 29 degrees of freedom.

In order to achieve economical program operation for cases where symmetrical occupant response is expected, an optional plane-motion model having 11 degrees of freedom is provided. Because of the potential for vertebral injury in aircraft accidents that involve a significant vertical component of impact velocity, some measure of vertebral loading was considered desirable in the occupant model. Therefore, the plane-motion model was configured to include beam elements in both the torso and neck, as shown in Fig. 2.

Presented as Paper 83-0926 at the AIAA/ASME/ASCE/AHS 24th Structures, Structural Dynamics and Materials Conference, Lake Tahoe, Nev., May 2-4, 1983; received May 31, 1983; revision received Jan. 3, 1984. Copyright © American Institute of Aeronautics and Astronautics, Inc., 1983. All rights reserved.

*Research Engineer. Member AIAA.

†Associate Professor, Mechanical and Aerospace Engineering. Member AIAA.

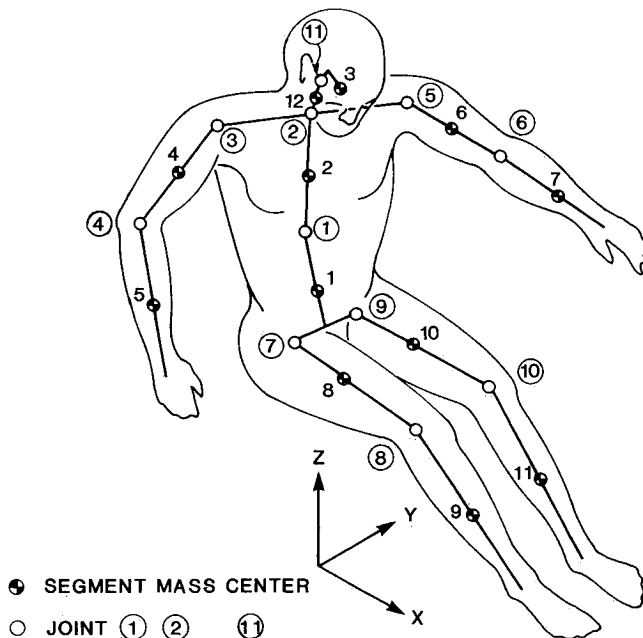


Fig 1 Twelve segment (three dimensional) occupant model

Resistance at each of the body joints is modeled using both a nonlinear torsional spring and a viscous torsional damper. The relative contributions of each of these elements can be varied to simulate either a human occupant or an anthropomorphic dummy. In modeling motion of the human body, resistance of the joints is controlled mostly by viscous damping, whereas resistance in dummy joints is dominated by a constant frictional torque.

The external forces that act on the 12 body segments can be characterized as either contact forces or restraint forces. The contact forces applied to the occupant are those forces exerted by the cushions and floor. They are calculated by first determining, from occupant displacement, the penetration of a rigid surface fixed to a body segment into either a cushion or the floor. To each of the normal forces computed from these penetrations, a damping term is applied which is proportional to the deflection rate. Friction forces are also applied by the seat bottom cushion and the floor. Each friction force is directed opposite to the tangential component of relative velocity between the occupant segment and the appropriate cushion or floor surface.

The restraint system consists of a lap belt which can be used alone or combined with a single or double strap shoulder harness. A lap belt tiedown strap also can be included. The restraint loads are transmitted to the occupant model through ellipsoidal surfaces fixed to the upper and lower torso segments. The belt loads are first calculated from the displacements of the torso segments, and the resultant force on each segment is then applied at the point along the arc of contact between the belt and the ellipsoidal surface where the force is normal to the surface. The capability of the point of application of the resultant belt loads to move relative to the torso surfaces allows simulation of submarining under the lap belt.

Seat Model

The seat structure is modeled using the finite element method of analysis. This method has been selected because it is not reliant on previous testing, and it has the flexibility to deal with a wide range of design concepts. The specific finite element formulation used in the program is based in part on the WRECKER II program, originally developed for automotive crash simulation.¹¹ The original version of the program was modified extensively to facilitate accurate and

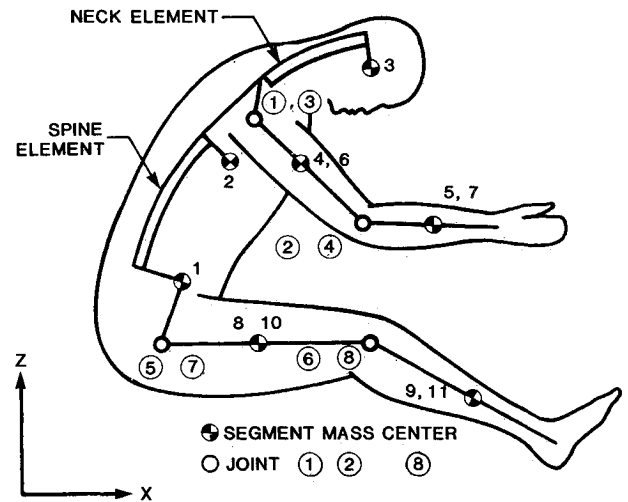


Fig 2 Eleven segment (symmetric) occupant model

economical analysis of aircraft seat structures.¹⁰ The element library includes triangular plate, three dimensional beam and spring elements. The seat model can accommodate large displacements, nonlinear material behavior and local buckling. Nonlinear material formulation is based on a uniaxial elastic-plastic stress strain law for beam and spring elements and a biaxial elastic plastic stress strain law (von Mises yield criterion) for plate elements. The large displacement formulation separates the element displacement field into a rigid body rotation and translation associated with a local coordinate system that moves with the element, and small element distortions relative to the current position of the element coordinate system. This formulation can accommodate extremely large rotations and deflections with accuracy depending on the size of the elements relative to the curvature of the structure.

Solution Procedure

The response of the seat model is determined from the formulation of the equations of quasistatic equilibrium in an incremental form as follows:

$$K_T(\dot{u}_{i+1} - \dot{u}_i) = \bar{F}_{i+1}^E - \bar{F}_i^E \quad \text{if } (\bar{F}_{i+1}^E - \bar{F}_i^E) > 0$$

$$= 0 \quad \text{if } (\bar{F}_{i+1}^E - \bar{F}_i^E) \leq 0 \quad (1)$$

where K_T is the tangent stiffness matrix, \bar{F}_i^E the external forces applied at i th solution time step, and \dot{u}_i the displacements (or rotations) at i th solution time step.

The external forces, \bar{F}^E including restraint system loads, occupant loads on the seat pan and seat back, and seat support reactions are treated as static loads on the seat structure. The mass of the seat structure is neglected since in most simulations it will be a small percentage of the occupant weight. The seat structure is assumed to be in a quasistatic equilibrium with the applied external forces \bar{F}^E .

During the period of the simulation when the external forces on the seat structure are increasing ($\bar{F}_{i+1}^E - \bar{F}_i^E > 0$), the incremental displacements ($\Delta \dot{u} = \dot{u}_{i+1} - \dot{u}_i$) are obtained from Eq (1). The total displacement of the seat structure is obtained by summation of the incremental displacements. However, when the external load(s) are decreasing ($\bar{F}_{i+1}^E - \bar{F}_i^E \leq 0$), the elastic unloading of the seat structure is neglected and the incremental displacement is assumed to be zero, ($\Delta \dot{u} = 0$) since in most simulations elastic deformations will be small compared with plastic deformations.

The tangent stiffness matrix K_T depends on the state of stress of the seat structure and varies with time during the

simulation. Therefore, it must be recomputed, assembled, and inverted at selected time steps during the simulation.

Coordinate Systems

Three different coordinate systems are used to describe the finite element model of the seat structure. They are global, nodal, and element coordinate systems.

The global coordinate system (x, y, z) is fixed in space and serves as an inertial frame of reference.

A nodal coordinate system ($\hat{x}, \hat{y}, \hat{z}$) is attached to each node. The orientation of nodal axes ($\hat{x}, \hat{y}, \hat{z}$) with respect to the global axes at any time is established by the components of three unit vectors $\hat{n}_1, \hat{n}_2, \hat{n}_3$ which remain fixed along the nodal axes ($\hat{x}, \hat{y}, \hat{z}$), respectively, as the node translates and rotates. If these three unit vectors $\hat{n}_1, \hat{n}_2, \hat{n}_3$ form the columns of a 3×3 matrix N , then any vector \bar{v} can be transformed from a nodal to a global coordinate system by the following time dependent transformation:

$$\bar{v}_G = N\bar{v}_N \quad (2)$$

An element coordinate system ($\hat{x}, \hat{y}, \hat{z}$) is attached to each element and serves to define the rigid body rotation and translation of the element. The orientation of the element axes ($\hat{x}, \hat{y}, \hat{z}$) with respect to the global axes at any time is established by the components of three unit vectors $\hat{e}_1, \hat{e}_2, \hat{e}_3$, which remain fixed along the element axes ($\hat{x}, \hat{y}, \hat{z}$), respectively, as the element translates and rotates. If the three unit vectors $\hat{e}_1, \hat{e}_2, \hat{e}_3$ form the columns of a 3×3 matrix E , then any vector \bar{v} can be transformed from an element to the global coordinate system by the following time dependent transformation:

$$\bar{v}_G = E\bar{v}_E \quad (3)$$

For triangular plate elements, the z axis is defined by the normal to the plane formed by the three corner nodes, and the x axis by a line bisecting the angle at a selected node (I), as shown in Fig. 3.

For beam elements the x axis is defined by a line connecting the end points of the beam, and the y axis by a line normal to the x axis and lying in a plane containing both a coordinate reference point and the x axis. The remaining z axis is determined as a normal to the x and y axes by the right hand rule.

For spring elements only one element axis is required, and it is defined by a line joining the end points of the spring.

Element Formulation

Large displacement formulation separates the element displacement field into rigid body rotation and translation and small element distortion relative to the current position of the element coordinate system. After the rigid body motion is removed it is possible to use the classical small deformation finite element formulation. Consequently, extremely large rotations and translations can be accommodated with accuracy depending on the size of the elements relative to the curvature of the deformed structure.

Beam Element

The beam element is based on the conventional small deflection formulation involving cubic shape functions for transverse displacements and linear shape functions for axial and torsional displacements.

From the principle of virtual work, the general form of the beam element tangent stiffness matrix is given by

$$K_T = \int_V D^T C D dV \quad (4)$$

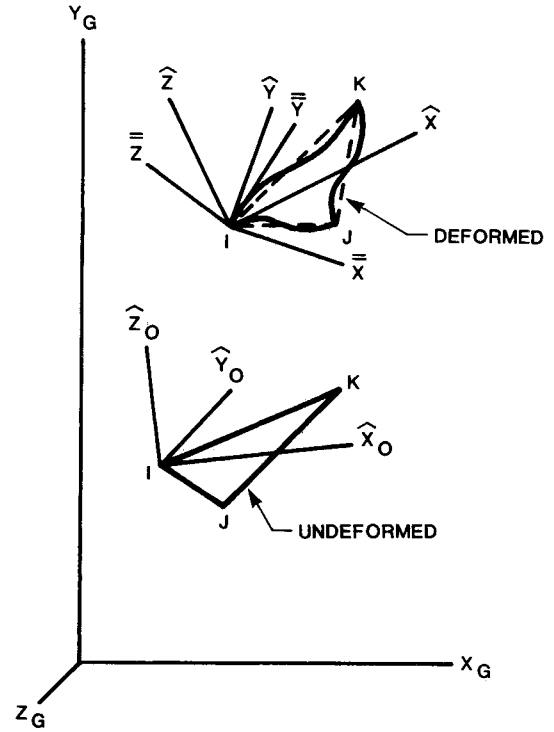


Fig. 3 Three dimensional plate element (from Ref. 11)

where K_T is the element tangent stiffness matrix, D the matrix that relates element strains to nodal displacements, and C the constitutive matrix that relates stresses and strains.

For nonlinear materials the coefficients of the constitutive matrix C are given by

$$C_{ij} = \Delta\sigma_{ij} / \Delta\epsilon_{ij} \quad (5)$$

where $\Delta\sigma_{ij}$ is the incremental stress and $\Delta\epsilon_{ij}$ the incremental strain.

Using the cubic shape functions for the transverse displacements and linear shape functions for axial and torsional displacements in matrix D , it can be shown that¹¹

$$K_T = \frac{1}{\ell^4} \int_0^\ell \begin{bmatrix} \alpha \ell^2 & -\beta_z \ell f_2 & \beta_y \ell f_2 & -\beta_z \ell f_1 & \beta_y \ell f_1 \\ \delta_z f_2^2 & -\delta_x f_2^2 & \delta_z f_3 & -\delta_x f_3 & \\ & \delta_y f_2^2 & -\delta_x f_3 & \delta_y f_3 & \\ & & \delta_z f_1^2 & -\delta_x f_1^2 & \\ & & & \delta_y f_1^2 & \end{bmatrix} d\ell \quad (6)$$

where ℓ is the element length and $f_1 = 6x - 2\ell$, $f_2 = 6x - 4\ell$, $f_3 = f_1 f_2$.

$$\begin{aligned} \alpha &= \int_A \frac{\Delta\sigma}{\Delta\epsilon} dA \\ \beta_y &= \int_A y \frac{\Delta\sigma}{\Delta\epsilon} dA & \beta_z &= \int_A z \frac{\Delta\sigma}{\Delta\epsilon} dA \\ \delta_x &= \int_A yz \frac{\Delta\sigma}{\Delta\epsilon} dA & \delta_y &= \int_A y^2 \frac{\Delta\sigma}{\Delta\epsilon} dA \\ \delta_z &= \int_A z^2 \frac{\Delta\sigma}{\Delta\epsilon} dA \end{aligned}$$

The integrals defined in Eq (6) are calculated numerically through the cross section and along the length of the beam element. The integration is piecewise linear through the depth and linear along the length.

Plate Element

The triangular plate element formulation is based on small deflection linear plate theory involving a linear displacement field of midplane deformations and a cubic displacement field for plate bending deformations.¹² Node point degrees of freedom are two in plane displacements u_x and u_y , and two rotations θ_x and θ_y . Nodal rotations normal to the plane of the plate θ_z are not admitted. The out of plane displacements u_z are zero since the x - y element coordinate plane is established by the deformed position of the nodes.

The development of the tangent stiffness matrix for plates is similar to the development for beams. The general form of the plate element stiffness matrix is the same as Eq (4)

$$K_T = \int_V D^T C D dV$$

where C is the constitutive matrix that relates the biaxial stresses and strains

$$C^T = \frac{\Delta\sigma_{xx}}{\Delta\epsilon_{xx}} \quad \frac{\Delta\sigma_{yy}}{\Delta\epsilon_{yy}} \quad \frac{\Delta\sigma_{xy}}{\Delta\epsilon_{xy}}$$

The triangular plate element elastic stiffness matrix is given in Ref. 12. For nonlinear materials, the stiffness matrix must be calculated by numerical integration based on the current state of stress and the plate strain displacement relations. This development is as follows.¹¹ The plate strains can be written as a combination of the membrane strains ϵ_{ij}^0 and curvature functions κ_{ij} in the form

$$\bar{\epsilon} = \begin{Bmatrix} \epsilon_{xx} \\ \epsilon_{yy} \\ \epsilon_{xy} \end{Bmatrix} = \begin{Bmatrix} \epsilon_{xx}^0 \\ \epsilon_{yy}^0 \\ \epsilon_{xy}^0 \end{Bmatrix} - z \begin{Bmatrix} \kappa_{xx} \\ \kappa_{yy} \\ \kappa_{xy} \end{Bmatrix} \quad (7)$$

or

$$\bar{\epsilon} = \phi \bar{u} - z \psi \bar{\theta}$$

where \bar{u} is the in plane displacements, $\bar{\theta}$ the plate corner rotations, ϕ the matrix of membrane strain functions¹² and ψ the matrix of curvature functions.¹¹

The complete strain displacement transformation matrix D has the form

$$D = \begin{bmatrix} \phi & 0 \\ 0 & -z\psi \end{bmatrix} \quad (8)$$

Introduction of this form of D into the stiffness matrix in Eq (4), results in

$$K_T = \begin{bmatrix} K_{uu} & K_{u\theta} \\ K_{\theta u} & K_{\theta\theta} \end{bmatrix} \quad (9)$$

where

$$\begin{aligned} K_{uu} &= \int_A \phi C_{uu} \phi^T dA \\ K_{u\theta} &= - \int_A \phi^T C_{u\theta} \psi dA \\ K_{\theta u} &= - \int_A \psi^T C_{\theta u} \phi dA \\ K_{\theta\theta} &= \int_A \psi^T C_{\theta\theta} \psi dA \end{aligned} \quad (10)$$

and

$$\begin{aligned} C_{uu} &= \int_{-h/2}^{h/2} C dz \\ C_{u\theta} &= C_{\theta u} = \int_{-h/2}^{h/2} z C dz \\ C_{\theta\theta} &= \int_{-h/2}^{h/2} z^2 C dz \end{aligned} \quad (11)$$

The matrices C_{uu} , $C_{u\theta}$, and $C_{\theta\theta}$ in Eq (11) are integrated numerically by the trapezoidal rule. For elastic materials $C_{u\theta}$ vanishes and hence,

$$K_{u\theta} = K_{\theta u} = 0$$

The integrals in Eq (10) are then evaluated numerically. These integrations involve cross sectional integrations carried out each time the stiffness matrix is created.

Material Nonlinearities

The nonlinear material formulation is based on a uniaxial elastic plastic stress strain law for beam and spring elements and a biaxial elastic plastic stress strain law (von Mises yield criterion) for plate elements.

The computational procedure for a biaxial stress field for plates is presented in Ref. 11 and is based on the work of Hartzman and Hutchinson,¹³ as specialized for small strain and plane stress conditions. The current stress state at a point in the plate is established as follows: Let the prior stress state of the point under consideration be σ_{xx}^0 , σ_{yy}^0 , σ_{xy}^0 and a small increment in strain from the prior state to the current state be $\Delta\epsilon_{xx}$, $\Delta\epsilon_{yy}$, $\Delta\epsilon_{xy}$. First, a tentative, current stress state $\bar{\sigma}_{xx} = \sigma_{xx}^0 + \Delta\sigma_{xx}$, $\bar{\sigma}_{yy} = \sigma_{yy}^0 + \Delta\sigma_{yy}$, $\bar{\sigma}_{xy} = \sigma_{xy}^0 + \Delta\sigma_{xy}$ is calculated as if the strain increment were completely elastic

$$\begin{aligned} \bar{\sigma}_{xx} &= \sigma_{xx}^0 + \frac{E}{1-\nu^2} (\Delta\epsilon_{xx} + \nu\Delta\epsilon_{yy}) \\ \bar{\sigma}_{yy} &= \sigma_{yy}^0 + \frac{E}{1-\nu^2} (\Delta\epsilon_{yy} + \nu\Delta\epsilon_{xx}) \\ \bar{\sigma}_{xy} &= \sigma_{xy}^0 + G\Delta\epsilon_{xy} \end{aligned} \quad (12)$$

where E is the modulus of elasticity, G the shear modulus and ν Poisson's ratio.

An effective stress $\bar{\sigma}_e$, to determine whether plastic flow has taken place during the strain increment, is calculated using the von Mises criterion

$$\bar{\sigma}_e = (\bar{\sigma}_{xx}^2 - \bar{\sigma}_{xx}\bar{\sigma}_{yy} + \bar{\sigma}_{yy}^2 + 3\bar{\sigma}_{xy}^2)^{1/2} \quad (13)$$

If $\bar{\sigma}_e$ is less than the prior effective stress σ_e^0 at which yielding occurred, elemental loads are decreasing and the tentative stresses calculated ($\bar{\sigma}_{xx}$, $\bar{\sigma}_{yy}$, $\bar{\sigma}_{xy}$) are the correct values of the

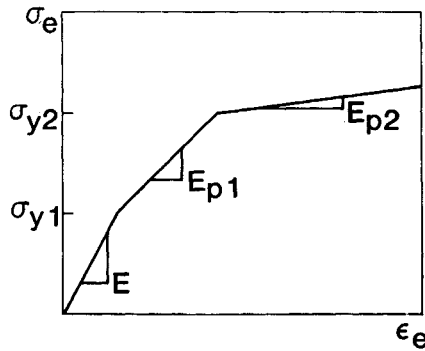


Fig. 4 Trilinear stress-strain relationship.

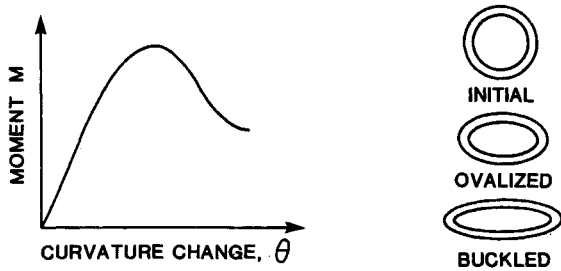


Fig. 5 Moment capability vs curvature for a thin-walled circular tube.

current stress values (σ_{xx} , σ_{yy} , σ_{xy}). If $\bar{\sigma}_e$ is greater than the prior effective stress σ_e^0 at which yielding occurred, tentative stresses calculated must be modified to account for the plastic behavior. Hartzman and Hutchinson¹³ have shown that the true value of the current effective stress will be

$$\sigma_e = \frac{\sigma_e^0 + \left(\frac{H'}{3G}\right)\bar{\sigma}_e}{1 + \left(\frac{H'}{3G}\right)} \quad (14)$$

where

$$H'_i = \frac{(E)(E_{pi})}{E - E_{pi}} \quad i=1,2$$

and E_{pi} is the plastic modulus (Fig. 4).

The current state of stress is then given by

$$\begin{aligned} \sigma_{xx} &= \frac{I}{I+3\lambda} [\bar{\sigma}_{xx} + \lambda(\bar{\sigma}_{xx} + \bar{\sigma}_{yy})] \\ \sigma_{yy} &= \frac{I}{I+3\lambda} [\bar{\sigma}_{yy} + \lambda(\bar{\sigma}_{xx} + \bar{\sigma}_{yy})] \\ \sigma_{xy} &= \frac{I}{I+3\lambda} \bar{\sigma}_{xy} \end{aligned} \quad (15)$$

where λ is given by

$$\lambda = \frac{I}{3} \left(\frac{\bar{\sigma}_e}{\sigma_e} - 1 \right) \quad (16)$$

The extension of the above formulation to uniaxial stress field for beam and spring elements is straightforward with $\sigma_{yy} = \sigma_{xy} = 0$.

Local Buckling of Beam Elements

Local buckling is one of the failure modes for thin-walled tubes typically used in light aircraft seats, when subjected to axial compressive and/or bending loads. The results of

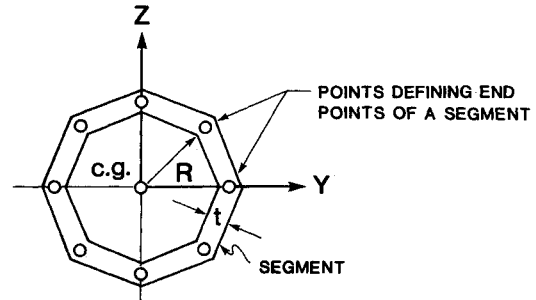
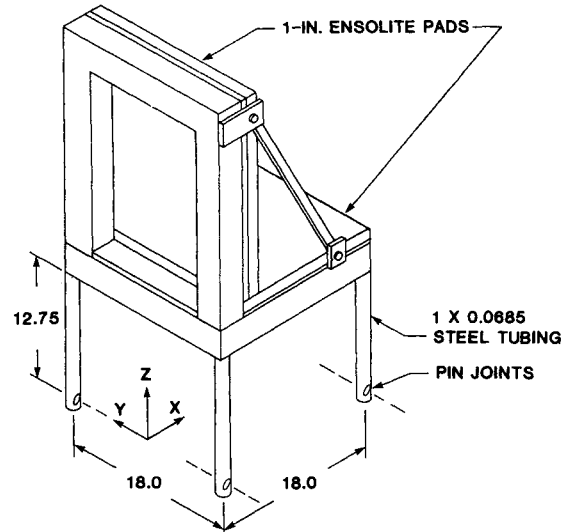


Fig. 6 Circular tube cross section defined by eight plate segments.



NOTE: ALL DIMENSIONS IN INCHES

Fig. 7 Validation test seat.

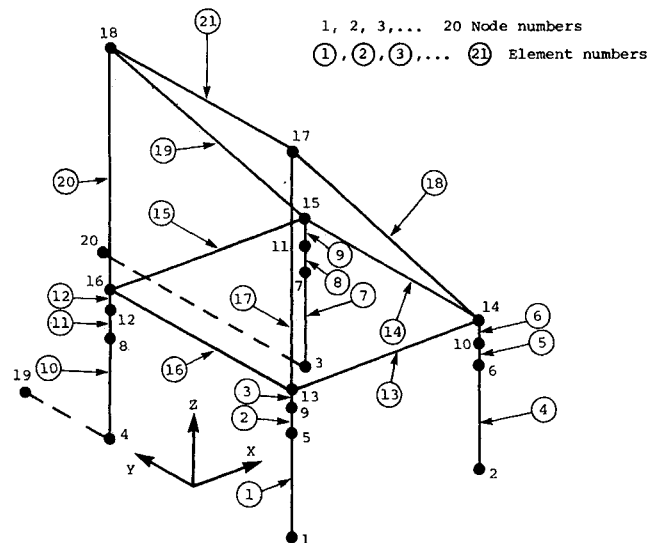


Fig. 8 Finite element model of test seat.

dynamic tests of aircraft seats have indicated that the local buckling of thin-walled tubes can have a significant effect on the response of the seat-occupant system. Therefore, a simple local buckling model for thin-walled tubes was incorporated into the program.

Local buckling is traditionally expressed in terms of a moment-curvature diagram, as shown in Fig. 5. The cross section goes through several stages of deformation as the structure bends. Although during this cross-sectional

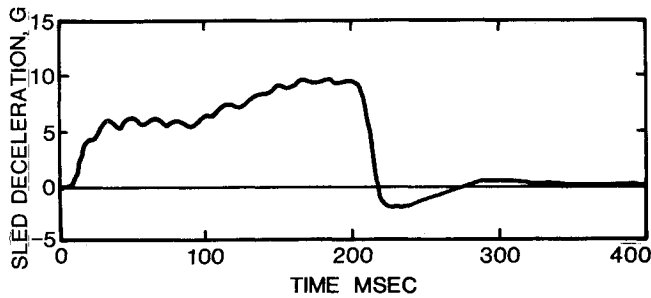


Fig 9 Sled deceleration, high deceleration tests

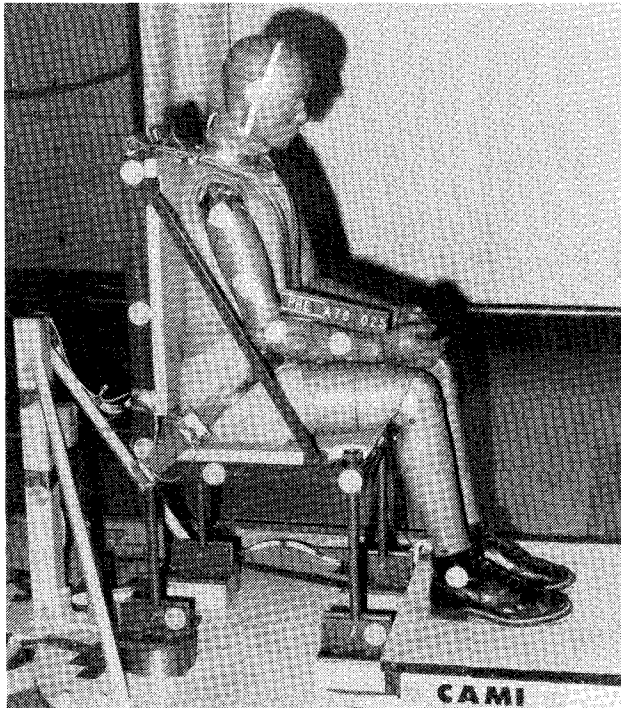


Fig 10 High deceleration test pretest

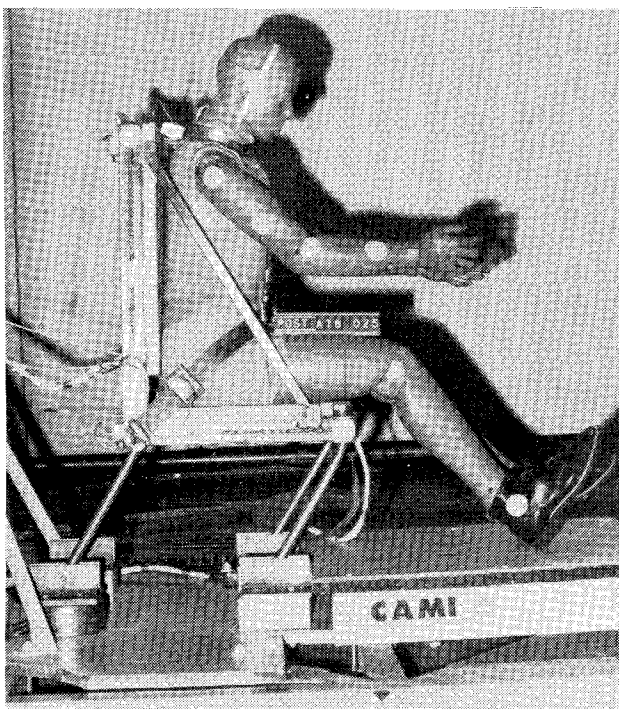


Fig 11 High deceleration test, post test

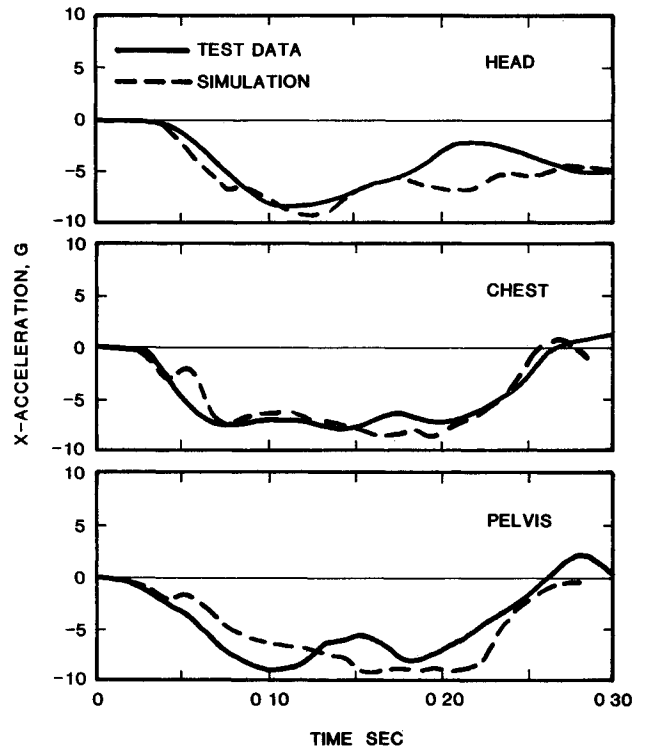


Fig 12 High deceleration validation tests; dummy head, chest, and pelvis x accelerations

distortion axial stresses redistribute themselves, it has been proposed¹⁴ that the reduced bending rigidity is related most strongly to the loss of lateral moment arm of the axial forces

The cross sections of beam elements are defined as thin walled segments by specifying their end points and thickness as part of the input data (Fig. 6). The tangent stiffness matrix for nonlinear beam elements is then computed by evaluating the integrals given in Eq (6) over the plate segments that define the beam cross section

The program computes the stresses at all integration points across the cross section at each end of the beam elements. These stresses are then compared with the local buckling stress σ_L for the beam element. If any of the compressive stresses at the integration points exceeds σ_L , the deformation of the cross section is modeled by modifying the radial location of that integration point using the following expression:

$$R_{i+1} = \left(\frac{\sigma_L}{|\sigma_{i+1}|} \right)^K R_i \quad \text{if } |\sigma_{i+1}| > \sigma_L \quad (17)$$

where R_i is the radial location of the integration point at time step i , σ_L the local buckling stress, σ_{i+1} the compressive stress at the integration point at time step $i+1$, and K the local buckling constant (0.50 recommended)

Consequently, reduced bending rigidity of the cross section due to the decrease in the lateral moment arm of axial forces during local buckling can be modeled

Model Validation

In order to validate the mathematical model several series of deceleration sled tests were performed at the Federal Aviation Administration Civil Aeromedical Institute (CAMI). Seats included a production energy absorbing helicopter seat and a production general aviation seat, the latter using a nonsymmetrical three point belt system. Test conditions and comparisons between measured data and simulation predictions are presented for all test series in Ref 10. The tests of greatest interest in validation of the seat model are described in detail in Ref 15. The seat structure consisted of a rigid seat pan and back braced at a 90 deg included angle, as

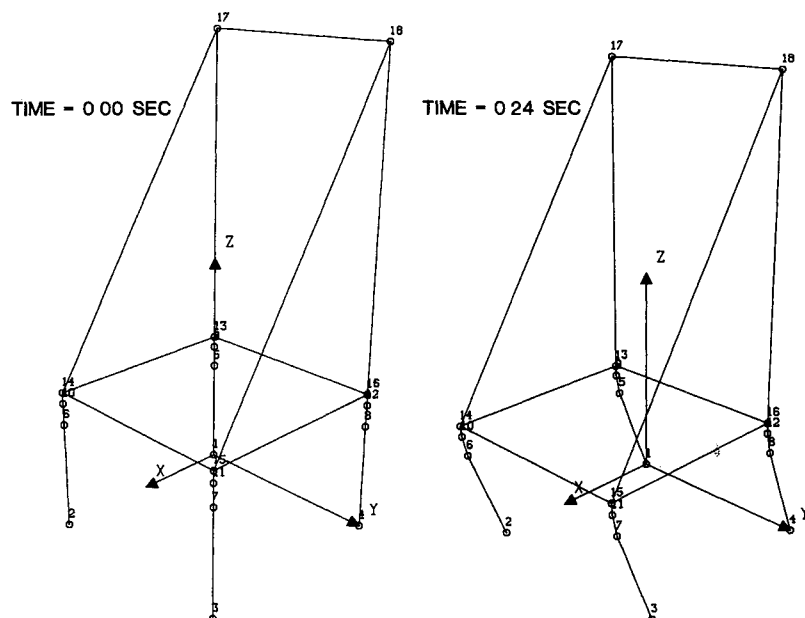


Fig 13 High deceleration test, initial and final seat positions

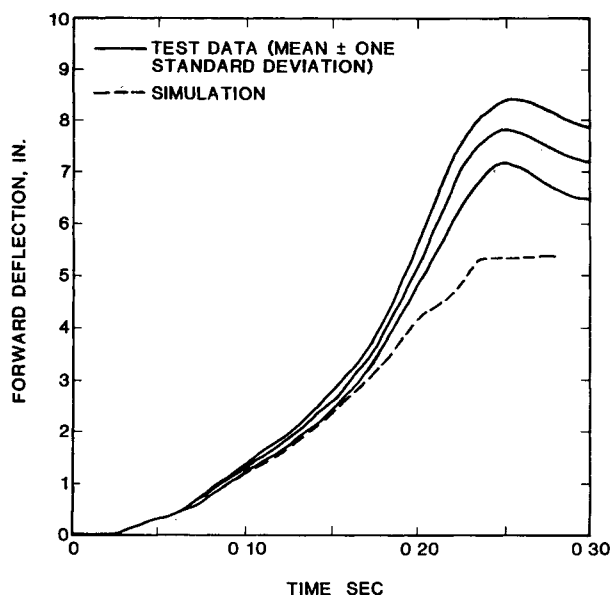


Fig 14 High deceleration tests, seat forward displacement

illustrated in Fig 7. The replaceable seat legs were 1 in. diam steel tubing with a wall thickness of 0.068 in., pin jointed at the bottom and fixed to the seat at the top. The cushions were 1 in. thick Ensolite pads on the seat pan and back, and the restraint system consisted of a conventional nylon lap belt attached to the seat frame with a double shoulder belt that was attached to the seat back and fitted to the buckle at the center of the belt. A finite element model of the simple seat structure is shown in Fig 8. Although two seat orientations were used, the configuration to be described here provided a purely forward facing ($-G_x$) deceleration. Two deceleration levels, 5.4 and 9.5 g, were used, and ten tests were conducted at each level. The lower deceleration level provided minimal plastic deformation of the legs without significant cross sectional change, while the higher deceleration level produced marked plastic deformation with localized buckling and cross sectional change at the fixed end.

The sled deceleration pulse used in the high deceleration tests is shown in Fig 9. Pre- and post-test photographs from one of the ten tests are shown in Figs 10 and 11. As shown in

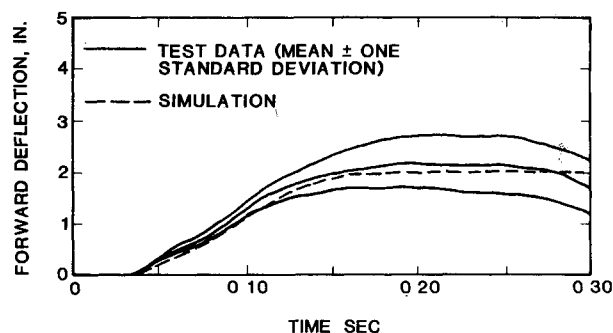


Fig 15 Low deceleration tests, seat forward displacement

the latter photograph, a significant forward displacement of the seat structure was achieved through plastic deformation and local buckling of the legs at their connection to the pan. Predicted dummy head, chest, and pelvis x accelerations are compared in Fig 12 with the mean of the data measured in ten tests. Initial and final seat positions are displayed in Fig 13 and predicted seat displacement is compared with test results in Fig 14.

As shown in Fig 14, the predicted displacement of the seat is approximately 2 in. less than that measured in the tests. The higher measured displacement was due mainly to the inertial loads associated with the relatively large mass of the seat structure. Inertial loads associated with the seat mass are neglected in the mathematical formulation because the general aviation type seats are typically much lighter than the replaceable leg test seat. As shown in Fig 15, a much better correlation between measured and predicted seat pan displacements was obtained in the low deceleration tests where the seat inertial loads were less significant.

Conclusions

A mathematical model of an aircraft seat and occupant has been developed for use in evaluation of the crashworthiness of seats and restraint systems in light aircraft. Although some further validation, particularly considering other types of

‡Program SOM LA is available from the FAA Technical Center, Atlantic City, N.J.

general aviation seat structures and nonsymmetrical loading is desirable, comparisons made to date of model predictions with test data have produced quite favorable results. These results indicate that the use of nonlinear finite element techniques have significant potential in crashworthiness analysis.

Acknowledgments

The final phase of development and validation was supported by the Federal Aviation Administration Technical Center under Contract DTFA03 80 C 00098. Testing was conducted by the Protection and Survival Laboratory of the FAA Civil Aeromedical Institute under the direction of Mr R F Chandler.

References

- ¹Laananen, D H, Aircraft Crash Survival Design Guide, Volume II, Aircraft Crash Environment and Human Tolerance, Applied Technology Laboratory, U S Army Research and Technology Laboratories (AVRADCOM) Fort Eustis Va USARTL TR-79 22B Jan 1980
- ²Twigg, D W and Karnes R N, PROMETHEUS—A User Oriented Program for Human Crash Dynamics Boeing Computer Services, Inc Seattle Wash Rept BCS 40038 Nov 1974
- ³Robbins D H Bowman B M. and Bennett R O, The MVMA Two Dimensional Crash Victim Simulation, *Proceedings of the Eighteenth Stapp Car Crash Conference* Society of Automotive Engineers Warrendale, Pa 1974 pp 657 678
- ⁴Young, R D A Three Dimensional Mathematical Model of an Automobile Passenger Texas Transportation Institute College Station Tex, Research Rept 140 2 1970
- ⁵Bartz J A., Development and Validation of a Computer Simulation of a Crash Victim in Three Dimensions *Proceedings of the Sixteenth Stapp Car Crash Conference*, Society of Automotive Engineers Warrendale Pa 1972 pp 105 127
- ⁶Robbins D H Bennett R O, and Bowman B M User Oriented Mathematical Crash Victim Simulation, *Proceedings of the Sixteenth Stapp Car Crash Conference* Society of Automotive Engineers Warrendale Pa 1972 pp 128 148
- ⁷Huston R L Hessel R and Passerello C A Three Dimensional Vehicle Man Model for Collision and High Acceleration Studies SAE Paper 740275 Society of Automotive Engineers Warrendale Pa 1974
- ⁸Maltha J and Wismans, J MADYMO—Crash Victim Simulations a Computerized Research and Design Tool, *Proceedings of the Vth International IRCOBI Conference* Birmingham, U K, International Research Committee on Biokinetics of Impacts Bron France 1980
- ⁹Laananen D H Development of a Scientific Basis for Analysis of Aircraft Seating Systems FAA RD 74 130 Jan 1975
- ¹⁰Laananen D H Bolukbasi A O and Coltman J W Computer Simulation of an Aircraft Seat and Occupant in a Crash Environment Volume I—Technical Report DOT/FAA/CT 82/33 I Sept 1982
- ¹¹Yeung, K S and Welch R E Refinement of Finite Element Analysis of Automotive Structures Under Crash Loading National Highway Traffic Safety Administration Washington D C DOT HS 803 466, Oct 1977
- ¹²Meek J L *Matrix Structural Analysis* McGraw Hill Book Co New York 1971
- ¹³Hartzman, M. and Hutchinson J R, Nonlinear Dynamics of Solids by the Finite Element Methods *Computers and Structures* Vol. 2 1972 pp 47 77
- ¹⁴Spunt L, *Optimum Structural Design* Prentice Hall Englewood Cliffs N J 1971
- ¹⁵Chandler R F and Laananen, D H Seat/Occupant Crash Dynamic Analysis Validation Test Program SAE Paper 790590 Society of Automotive Engineers Warrendale Pa April 1979

From the AIAA Progress in Astronautics and Aeronautics Series

ALTERNATIVE HYDROCARBON FUELS: COMBUSTION AND CHEMICAL KINETICS—v. 62

A Project SQUID Workshop

*Edited by Craig T Bowman Stanford University
and Jørgen Birkeland Department of Energy*

The current generation of internal combustion engines is the result of an extended period of simultaneous evolution of engines and fuels. During this period the engine designer was relatively free to specify fuel properties to meet engine performance requirements and the petroleum industry responded by producing fuels with the desired specifications. However today's rising cost of petroleum coupled with the realization that petroleum supplies will not be able to meet the long term demand has stimulated an interest in alternative liquid fuels particularly those that can be derived from coal. A wide variety of liquid fuels can be produced from coal and from other hydrocarbon and carbohydrate sources as well ranging from methanol to high molecular weight low volatility oils. This volume is based on a set of original papers delivered at a special workshop called by the Department of Energy and the Department of Defense for the purpose of discussing the problems of switching to fuels producible from such nonpetroleum sources for use in automotive engines aircraft gas turbines and stationary power plants. The authors were asked also to indicate how research in the areas of combustion fuel chemistry and chemical kinetics can be directed toward achieving a timely transition to such fuels should it become necessary. Research scientists in those fields as well as development engineers concerned with engines and power plants will find this volume a useful up to date analysis of the changing fuels picture.

463 pp 6×9 illus \$20 00 Mem \$35 00 List

TO ORDER WRITE: Publications Order Dept AIAA 1633 Broadway New York N Y 10019